Overcoming the limits of vortex formation in magnetic nanodots by coupling to antidot matrix

R. V. Verba,[1,2,*] D. Navas,[1] A. Hierro-Rodriguez,[1,3] S. A. Bunyaev,[1]
B. A. Ivanov,[2,4] K. Y. Guslienko,[5,6] and G. N. Kakazei[1]

[1] *IFIMUP-IN/Departamento de Fisica e Astronomia, Universidade do Porto, 4169-007 Porto, Portugal*
[2] *Institute of Magnetism, Kyiv 03680, Ukraine*
[3] *SUPA, School for Physics and Astronomy, University of Glasgow, Glasgow, G12 8QQ, UK*
[4] *National University of Science and Technology "MISiS", Moscow, 119049, Russian Federation*
[5] *Depto. Física de Materiales, Universidad del País Vasco, UPV/EHU, 20018 San Sebastián, Spain*
[6] *IKERBASQUE, the Basque Foundation for Science, 48013 Bilbao, Spain*

(Dated: August 28, 2018)

Static magnetic configurations of thin circular soft (permalloy) magnetic nanodots, coupled to a hard antidot matrix with perpendicular magnetization, are studied by micromagnetic simulations. It is demonstrated, that dipolar fields of the antidot matrix promotes the formation of a magnetic vortex state in nanodots. The vortex is the dot ground state at zero external field in ultrathin nanodots with diameters as low as 60 nm, that is far beyond the vortex stability range in an isolated permalloy nanodot. Depending on the geometry and antidot matrix material it is possible to stabilize either radial vortex state or unconventional vortices with the angle between in-plane magnetization and radial direction $\psi \neq 0, \pi/2$.

Magnetic vortices are one of the simplest topologically nontrivial configurations which can be achieved in ferromagnetic films and nanostructures [1–3]. They were extensively investigated during past two decades both from fundamental point and in the relation with applications in magnetic recording [4–6], microwave applications, including magnonic crystals [7, 8] and high-power vortex spin-torque oscillators [9–11], medicine [12], etc. For several applications it is desirable to stabilize magnetic vortex in a nanodot with the smallest possible thickness and lateral dimensions. For example, spin-transfer torque efficiency in magnetic-tunnel-junction-based spin-torque oscillators is inversely proportional to the thickness [10], usage of novel interface effects like voltage-controlled magnetic anisotropy [13, 14], spin-Hall effect [15, 16], interfacial Dzyaloshinskii-Moriya interaction [17, 18], which may increase functionality and efficiency of vortex-based devices, also requires thickness less than 5 nm. A decrease of lateral sizes results in higher frequencies of vortex excitations [2] and allows to enhance integrability.

However, in the simplest and the most studied geometry – thin circular nanodot, made of soft magnetic material, vortex state can be realized only in relatively large dots, while smaller ones exist in a quasi-uniform single-domain state. The minimal dot diameter, required to make vortex state the ground one (state corresponding to the global magnetic energy minimum) at zero external field, inversely depends on the dot thickness [19, 20]. For example, for commonly used soft ferromagnetic Permalloy ($Ni_{80}Fe_{20}$) of the thickness $t_\mathrm{d} = 10\,\mathrm{nm}$ the minimal diameter is about $d_\mathrm{d} = 80$ nm, for $t_\mathrm{d} = 5\,\mathrm{nm}$ it is 160 nm [19]. However, metastability of quasi-uniform state in a large area close to the geometrical parameters, at which vortex state becomes the ground state [20], complicates observation and usage of vortices in this range, since it is impossible to nucleate a vortex by bias field decrease from in-plane or out-of-plane saturation. To guarantee vortex appearance, the single-domain state should become unstable in zero field. This case is realized if the dot thickness is larger than $t_\mathrm{d} \gtrsim 30\pi\lambda_{ex}^2/d_\mathrm{d}$ [20], where λ_{ex} is the material exchange length ($\lambda_{ex} \approx 5.5\,\mathrm{nm}$ for Permalloy), i.e. $t_\mathrm{d} > 14\,\mathrm{nm}$ for 200 nm diameter and $t_\mathrm{d} > 28\,\mathrm{nm}$ for $d_\mathrm{d} = 100\,\mathrm{nm}$. For this reason almost all the experiments were performed for the dot thickness $t_\mathrm{d} > 10\,\mathrm{nm}$ [21]. An exception is vortex spin-torque oscillators, in which Oersted field of bias current promotes the vortex formation and solves the problem with metastable quasiuniform state, making possible the operation with 5-10 nm thick free layers [9–11].

In this Letter we show how to achieve vortex ground state in much smaller nanodots with ultrathin thickness and diameters down to 50 nm and how to switch a dot into a vortex state in the region, where it is metastable. Our approach is based on the dipolar coupling of a soft magnetic nanodot with perpendicularly magnetized antidot matrix, dipolar stray fields of which have necessary radial symmetry and promotes vortex formation.

There are different types of magnetic vortices. In general, two-dimensional vortex is the topologically nontrivial magnetization configuration with winding number $\nu = 1$ [22]. Magnetization distribution away from the vortex core is determined by $\phi = \chi + \psi$, where ϕ is the azimuthal angle of magnetization (i.e. $M_x/M_s = \cos\phi$, $M_y/M_s = \sin\phi$), χ is the azimuthal coordinate in polar coordinate system, and ψ – parameter determining vortex structure. In the most of cases vortices with $\psi = \pm\pi/2$, which have closure-flux structure, were stud-

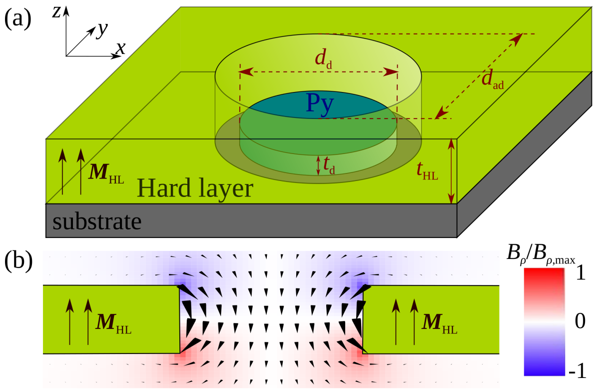

FIG. 1. (a) A sketch of the considered nanostructure – soft magnetic nanodot placed within an antidot in hard magnetic layer with perpendicular magnetization. (b) - Distribution of stray fields in the antidot; arrow length corresponds to the field magnitude, color – to the field radial component B_ρ.

ied. Properties of such vortices were investigated in easy-plane anisotropic films [1], in thin circular nanodots, including static properties [19, 20, 23], linear (see Ref. 2 and references therein) and nonlinear [24–26] dynamics, in nanodot arrays [7, 27], relatively thick nanodots [28, 29], stacked two-dot systems [30] and in other more complex geometries. Vortices with other values of ψ are often called "unconventional vortices" [31]. For $\psi = 0, \pi$ these are "radial vortices", which were observed in ultrathin nanodots with interfacial Dzyaloshinskii-Moriya interaction [32], pairs of nanodots with antiferromagnetic exchange coupling [33, 34] and at the crosses of ferromagnetic nanowires [31]. Vortices with $\psi \neq 0, \pm\pi/2, \pi$ are realized in thick circular nanodots (however, their structure is thickness-dependent) [29, 31]. Interestingly, that unconventional vortices were proposed as pinned layer in skyrmion-based spin-torque oscillator and revealed characteristics which cannot be achieved by using common vortices [35].

The patterned film under consideration is shown in Fig. 1. It is a layer of hard magnetic material with perpendicular magnetization of the thickness t_{HL}, having an antidot of the diameter d_{ad}. Inside an antidot there is a nanodot of the thickness t_{d} and diameter d_{d}, made of soft magnetic material. The dot is grown on the same substrate as hard magnetic layer, resulting in asymmetric vertical position of the dot respective to the hard layer. We assume that the direct exchange coupling between dot and hard layer is absent, that is the case, e.g., if the dot diameter is smaller than the antidot diameter, as shown in Fig. 1(a). Below we use 10 nm difference between diameters of the antidot and dot.

The magnetization distribution in the nanostructure was studied using MuMax3 micromagnetic solver [36]. As a dot material we choose Permalloy (saturation magnetization $M_s = 8.1 \times 10^5$A/m, exchange stiffness $A = 1.05 \times 10^{-11}$ J/m); parameters of hard magnetic layer were set as $M_s = 10^6$ A/m, $A = 2 \times 10^{-11}$ J/m, constant of uniaxial perpendicular anisotropy $K_u = 7 \times 10^5$ J/m^3, which correspond to FePd, FePt, CoPt multilayers of different composition. Strictly speaking, the only important characteristic of hard layer for the studied case is M_s, while anisotropy should be simply strong enough to guarantee stable perpendicular magnetization state in zero field. The minimal required anisotropy, in a general case, depends on the antidot lattice geometry [37, 38]. Our simulations confirm stable quasi-uniform OOP magnetization in zero field (after perpendicular saturation) in the whole studied range for chosen material parameters. Notes on different hard layer magnetization, as well as on different location of a dot will be given below. The cell size was chosen to be $2.5 \times 2.5 \times 1.5\,\text{nm}^3$, and $1.25 \times 1.25 \times 1\,\text{nm}^3$ for the smallest dots. To avoid edge effects we set periodic boundary conditions with period 400 nm, which is large enough to not produce interdot interaction.

The perpendicularly magnetized hard layer creates magnetostatic stray fields inside the antidot and in its vicinity. The stray fields are radially symmetric and have radial B_ρ and perpendicular B_z components (Fig. 1(b)). The radial component is zero at the central plane and reaches maximum close to the top and bottom hard layer surfaces.

Firstly we consider the effect of the hard layer thickness, fixing the dot thickness to $t_{\text{d}} = 3\,\text{nm}$, and investigating the dot remanent states which appear after perpendicular saturation by external field $\boldsymbol{B} = B_z \boldsymbol{e}_z$ and then gradual decrease of the field to zero. In the case $t_{\text{HL}} = t_{\text{d}}$ the averaged over the dot thickness radial component of stray fields is zero, and we observe quasi-uniform single-domain "leaf-like" state (Fig. 3(a)) in all the simulation range (Fig. 2). It is expected, as for an isolated dot of the thickness $t_{\text{d}} = 3\,\text{nm}$ single-domain state is the ground one up to approximately 235 nm dot diameter and remains stable up to 1 micron dot diameter. Therefore, the vortex nucleation in an isolated dot of such thickness is almost impossible.

However, as soon as t_{HL} increases, the radial component of stray field becomes nonzero and we start observe vortex state at remanence. With an increase of the hard layer thickness vortex state becomes more and more favorable and for $t_{\text{HL}} = 39\,\text{nm}$ we observe it even for 50 nm nanodot diameter (Fig. 2).

Note, that in all the cases the remanent state is "unconventional" vortex. For strong enough stray field emanated by the matrix (large matrix thickness) Zeeman energy of dot magnetization in stray field dominates and the radial vortex is formed (Fig. 3(c)). The radial vortex has small core region with out-of-plane magnetization and in-plane part with divergent ($\psi = 0$) or convergent ($\psi = \pi$) to the center magnetization. The direction of in-plane part depends, naturally, on the magnetization of

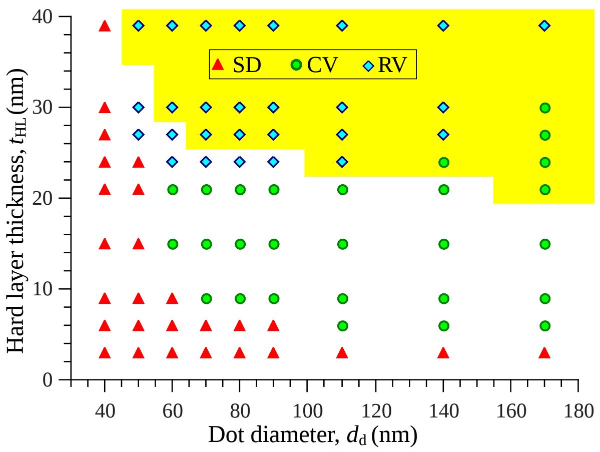

FIG. 2. Diagram of the magnetization remanent states of nanodot of the thickness $t_{\rm d} = 3\,$nm: SD – single-domain state, CV – curled vortex, RV – radial vortex. Yellow filled area shows the region, where vortex state is the ground state.

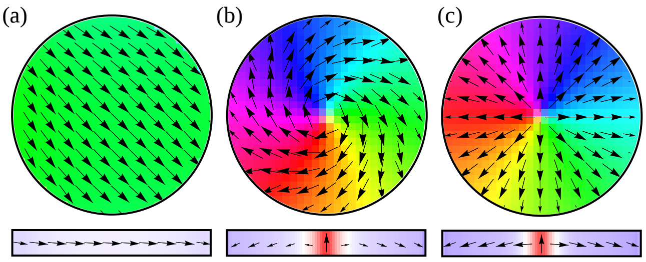

FIG. 3. Magnetization configuration of the 70 nm diameter dot in: (a) single-domain state (hard layer thickness $t_{\rm HL} = 6\,$nm), (b) curled vortex state ($t_{\rm HL} = 15\,$nm), and (c) radial vortex state ($t_{\rm HL} = 24\,$nm); up – top view, bottom – y-z cross-section; dot thickness $t_{\rm d} = 3\,$nm.

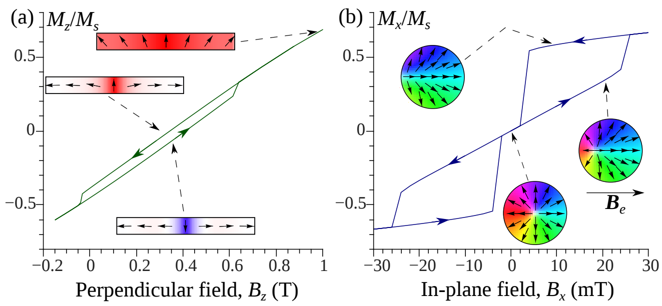

FIG. 4. Out-of-plane (a) and in-plane (b) hysteresis loops of nanodot in the vortex ground state and corresponding magnetization distributions. Dot diameter $d_{\rm d} = 90\,$nm, dot thickness $t_{\rm d} = 3\,$nm, hard layer thickness $t_{\rm HL} = 30\,$nm. For the plots only magnetization of the dot is accounted.

matrix. In our case $M_{z,{\rm HL}}/M_s = +1$, the matrix creates divergent radial field at the bottom resulting in divergent magnetization of the vortex. If one reverses the matrix magnetization or place the dot on matrix top, the vortex structure will be convergent.

With a decrease of the hard layer thickness or/and an increase of the dot diameter, the demagnetization energy becomes more important and it competes with Zeeman energy, resulting in the formation of curled unconventional vortex. It is characterized by $\psi \neq 0, \pm\pi/2, \pi$, which, strictly speaking, depends on the distance form the dot center $\psi = \psi(\rho)$ (see example in Fig. 3(b)). The value of ψ changes gradually with geometrical parameters, in particular, in the limit $d_{\rm d} \gg t_{\rm HL}$ the vortex structure is transformed to conventional vortex with $\psi = \pm\pi/2$. Thus, the proposed approach gives ability to tune the vortex structure and achieve unconventional vortices with given ψ, that can be necessary, e.g., for skyrmion-based spin-torque oscillators [35]. It should be also noted that in both cases of radial and curled vortices their out-of-core regions have small perpendicular component due to influence of perpendicular stray field of antidot matrix. This component disappears at certain nonzero external field $B_z \neq 0$.

We have checked if the vortex state is the ground one by comparison of its energy in zero field with the energy of single-domain state, which was manually introduced and allowed to relax into local energy minimum. The corresponding region of vortex ground state is smaller than the region, where vortex state was achieved at remanence (Fig. 2). However, sufficiently thick matrix allows to make vortex configuration the ground state in dots with diameters well below 100 nm. For practical applications it is desirable, of course, to work in this vortex ground state region. However, outside of this region a vortex can be also nucleated in practice by the decrease of external field from perpendicular saturation, as was done in simulations. It happens because stray fields of antidot promote the radial vortex formation, which then may transform to curled vortex, when B_z is gradually decreased. Due to the energy barriers between the vortex and saturated states [39, 40] the vortex state remains stable at remanence. Only in the region where vortex state is unstable respective to small perturbations one cannot observe it (single-domain region in Fig. 2). It is in contrast to the case of an isolated dot, where uniform bias field does not help the vortex formation and single-domain state remains at zero field in the metastability range.

As in the case of common vortex [41], the core polarity of unconventional vortices can be switched by perpendicular external magnetic field. The corresponding hysteresis loop is, of course, shifted respective to zero field (Fig. 4(a)) due to the influence of perpendicular component of the antidot stray field. This shift is more pronounced for thicker matrices, and for a sufficiently thick matrix, both switching fields can be positive, meaning that only state with the core polarity opposite to the matrix magnetization remains stable at zero bias field.

The behavior of unconventional vortices in an in-plane

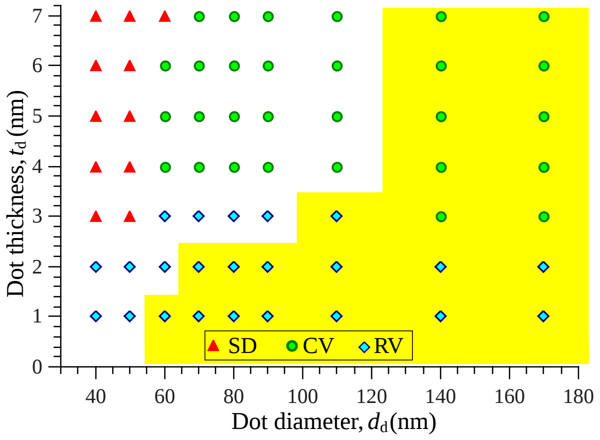

FIG. 5. Diagram of the magnetization remanent states of nanodot in the antidot matrix of the thickness $t_{\rm HL} = 24\,$nm; notation as in Fig. 2.

bias field is also similar to that for common vortex [23]. The corresponding hysteresis loop has characteristic "double-triangle" shape, vortex is expelled from the dot at annihilation field and nucleates when field decreases to nucleation field (Fig. 4(b)). Naturally, the core polarity of nucleated vortex is opposite to the matrix magnetization, as it is energy favorable. Under in-plane applied field the core of radial vortex moves in opposite to the field direction (see insets in Fig. 4(b)), while the core of curled vortex moves at some finite angle ($\neq \pi/2$) to the field direction. In contrast, the core of common vortex moves perpendicularly to the field [23]. This different behavior is a consequence of different distributions of in-plane part of vortex magnetization. Thus, one can nucleate and manipulate vortices in the considered nanoscale dots by relatively small in-plane magnetic fields (of course, if the matrix is magnetized perpendicularly before). However, this method works only in the region of vortex ground state. Outside of it vortex does not nucleate after in-plane saturation of nanodot.

Next we investigate the role of the Permalloy dot thicknesses t_d. To do this, we fix the hard layer thickness to $t_{\rm HL} = 24\,$nm and perform simulations for different values of t_d. As one can see from the states diagram (Fig. 5), with a decrease of the dot thickness vortex state become the ground state in smaller dots, that is the opposite tendency to that for an isolated dot. Also, for thinner dots the formation of radial vortices becomes more favorable. These features are related with the reduction of demagnetization energy of the radial vortex state with a decrease of the thickness-to-diameter aspect ratio of the dot.

As it is clear from the consideration above the main impact of antidot matrix is radial component of stray fields, which it creates. Within the antidot at the top/bottom of hard layer this component is approximately equal to

$$B_\rho \approx \pm\mu_0 M_{s,\rm HL}\frac{\rho}{2d_{\rm ad}}\left(1-\left[1+\frac{2t_{\rm HL}}{d_{\rm ad}}\right]^{-3/2}\right), \qquad (1)$$

where ρ is the distance from the antidot center (this estimation assumes $t_{\rm d} \ll t_{\rm HL}$ and is valid for $\rho < d_{\rm ad}/2$ except the region close to the antidot edge). B_ρ is proportional to the saturation magnetization of the hard layer and to its thickness (up to $t_{\rm HL} >> d_{\rm ad}$, where it saturates). Thus, one may reduce the hard layer thickness by using materials with higher M_s, or use materials with lower M_s and sufficiently large thickness. The behavior of the dot is the same if B_ρ is fixed. Also, it is clear that one can place a dot in other way, than shown in Fig. 1(a). For example, dot of smaller, equal, or slightly larger diameter than antidot can be placed on the top of antidot matrix. The only requirements are presence of radial stray fields and absence of exchange coupling between dot and matrix, which may drastically affect magnetization distribution in a dot.

In conclusion, we have demonstrated that dipolar coupling with perpendicularly magnetized antidot matrix can substantially enlarge the region of vortex stability in soft magnetic circular nanodots to the range of ultrathin thicknesses and sub-100 nm diameters. The main impact is produced by the radial component of antidot stray field, which leads to the appearance and stabilization of the magnetic vortices with unconventional texture. The vortex magnetization configuration can be tuned by a proper choice of geometrical parameters of the patterned film. In the case of sufficiently thick matrix and thin dots the radial vortices are formed, and unconventional curled vortices with the angle between in-plane magnetization and radial direction $\psi \neq 0, \pm\pi/2, \pi$ are stabilized otherwise. The vortices can be nucleated by the magnetic field decrease staring from perpendicular saturated state and, except the range of vortex metastability, starting from in-plane saturated state provided perpendicular single-domain state of antidot matrix.

The application of proposed nanostructures could significantly improve characteristics of vortex-based spintronic devices, e.g. vortex spin-torque oscillators. Indeed, thinner free layers, 2-3 nm in thickness, allow reducing bias current density in 3-5 times compared to commonly used isolated vortex-state dots with 10-20 nm thickness. Small dot diameters together with the presence of additional restoring force coming from matrix stray field result in a higher frequency of gyrotropic mode of the vortex. For example, in preliminary simulations for 3 nm dot thickness and $t_{\rm HL} = 39\,$nm we observed the gyrotropic mode frequency as high as 1-1.5 GHz. Such frequencies can be accessed in isolated dots of the thickness about 50 nm [29, 42], which are incompatible with spin-transfer-torque based devices. Of course, the detailed study of dynamic properties of the nanostructure is a topic for separate work. Finally, stabilization of unconventional vortices is important for skyrmion-based spin-torque oscillators [35].

The Portuguese team acknowledges the Network of Extreme Conditions Laboratories-NECL and Portuguese Foundation of Science and Technology (FCT) support through the projects NORTE-01-0145-FEDER-022096, MIT-EXPL/IRA/0012/2017, EXPL/IF/01191/2013 (D.N.), EXPL/IF/00541/2015 (S.A.B.), EXPL/IF/00981/2013 (G.N.K), SFRH/BPD/90471/2012(A.H.-R.). Work was also supported by: the Ministry of Education and Science of Ukraine, project No. 0118U004007 (R.V.V., B.A.I.); IKERBASQUE (the Basque Foundation for Science) (K.Y.G.); the Spanish MINECO, grants FIS2016-78591-C3-3-R (K.Y.G.), FIS2016-76058-C4-4-R (A.H.-R.); the European Union Horizon 2020 Research and Innovation Programme under Marie Skłodowska-Curie Grant Agreement No. 644348 (R.V.V., B.A.I., K.Y.G.) and No. H2020-MSCA-IF-2016-746958 (A.H.-R.). B.A.I. was supported by the Program of NUST "MISiS" (grant No. K2-2017-005), implemented by a governmental decree No. 211 dated 16 March 2013. G.N.K. acknowledges the support from European Cooperation in Science and Technology (COST) project CA16218 "NANOCOHYBRI".

* corresponding author, e-mail: verrv@ukr.net

[1] D. L. Huber, "Dynamics of spin vortices in two-dimensional planar magnets," Phys. Rev. B **26**, 3758–3765 (1982).

[2] K. Yu. Guslienko, "Magnetic Vortex State Stability, Reversal and Dynamics in Restricted Geometries," J. Nanosci. Nanotechnol. **8**, 2745–2760 (2008).

[3] R. Antos, Y. Otani, and J. Shibata, "Magnetic Vortex Dynamics," J. Phys. Soc. Japan **77**, 031004 (2008).

[4] B. Van Waeyenberge, A. Puzic, H. Stoll, K. W. Chou, T. Tyliszczak, R. Hertel, M. Fahnle, H. Bruckl, K. Rott, G. Reiss, I. Neudecker, D. Weiss, C. H. Back, and G. Schutz, "Magnetic vortex core reversal by excitation with short bursts of an alternating field," Nature **444**, 461–464 (2006).

[5] R. Hertel, S. Gliga, M. Fähnle, and C. M. Schneider, "Ultrafast nanomagnetic toggle switching of vortex cores," Phys. Rev. Lett. **98**, 117201 (2007).

[6] M. Kammerer, M. Weigand, M. Curcic, M. Noske, M. Sproll, A. Vansteenkiste, B. Van Waeyenberge, H. Stoll, G. Woltersdorf, C. H. Back, and G. Schuetz, "Magnetic vortex core reversal by excitation of spin waves," Nat. Commun. **2**, 279 (2011).

[7] A. A. Awad, K. Y. Guslienko, J. F. Sierra, G. N. Kakazei, V. Metlushko, and F. G. Aliev, "Spin excitation frequencies in magnetostatically coupled arrays of vortex state circular Permalloy dots," Appl. Phys. Lett. **96**, 012503 (2010).

[8] D.-S. Han, A. Vogel, H. Jung, K.-S. Lee, M. Weigand, H. Stoll, G. Schütz, P. Fischer, G. Meier, and S.-K. Kim, "Wave modes of collective vortex gyration in dipolar-coupled-dot-array magnonic crystals," Sci. Rep. **3**, 2262 (2013).

[9] R. Lehndorff, D. E. Bürgler, S. Gliga, R. Hertel, P. Grünberg, C. M. Schneider, and Z. Celinski, "Magnetization dynamics in spin torque nano-oscillators: Vortex state versus uniform state," Phys. Rev. B **80**, 054412 (2009).

[10] A. Dussaux, B. Georges, J. Grollier, V. Cros, A.V. Khvalkovskiy, A. Fukushima, M. Konoto, H. Kubota, K. Yakushiji, S. Yuasa, K.A. Zvezdin, K. Ando, and A. Fert, "Large microwave generation from current-driven magnetic vortex oscillators in magnetic tunnel junctions," Nat. Commun. **1**, 8 (2010).

[11] S. Tsunegi, H. Kubota, K. Yakushiji, M. Konoto, S. Tamaru, A. Fukushima, H. Arai, H. Imamura, E. Grimaldi, R. Lebrun, J. Grollier, V. Cros, and Shinji Yuasa, "High emission power and Q factor in spin torque vortex oscillator consisting of FeB free layer," Appl. Phys. Express **7**, 063009 (2014).

[12] D.-H. Kim, E. A. Rozhkova, I. V. Ulasov, S. D. Bader, T. Rajh, M. S. Lesniak, and V. Novosad, "Biofunctionalized magnetic-vortex microdiscs for targeted cancer-cell destruction," Nat. Mater. **9**, 165 (2010).

[13] M. Weisheit, S. Fähler, A. Marty, Y. Souche, C. Poinsignon, and D. Givord, "Electric field-induced modification of magnetism in thin-film ferromagnets," Science **315**, 349 (2007).

[14] C.-G. Duan, J. P. Velev, R. F. Sabirianov, Z. Zhu, J. Chu, S. S. Jaswal, and E. Y. Tsymbal, "Surface magnetoelectric effect in ferromagnetic metal films," Phys. Rev. Lett. **101**, 137201 (2008).

[15] K. Ando, S. Takahashi, K. Harii, K. Sasage, J. Ieda, S. Maekawa, and E. Saitoh, "Electric manipulation of spin relaxation using the spin Hall effect," Phys. Rev. Lett. **101**, 036601 (2008).

[16] V. E. Demidov, S. Urazhdin, H. Ulrichs, V. Tiberkevich, A. Slavin, D. Baither, G. Schmitz, and S. O. Demokritov, "Magnetic nano-oscillator driven by pure spin current," Nat. Mater. **11**, 1028 (2011).

[17] M. Bode, M. Heide, K. von Bergmann, P. Ferriani, S. Heinze, G. Bihlmayer, A. Kubetzka, O. Pietzsch, S. Blügel, and R. Wiesendanger, "Chiral magnetic order at surfaces driven by inversion asymmetry," Nature **447**, 190 (2007).

[18] L. Udvardi and L. Szunyogh, "Chiral asymmetry of the spin-wave spectra in ultrathin magnetic films," Phys. Rev. Lett. **102**, 207204 (2009).

[19] K. L. Metlov and K. Yu. Guslienko, "Stability of magnetic vortex in soft magnetic nano-sized circular cylinder," J. Magn. Magn. Matter. **242-245**, 1015 (2002).

[20] K. L. Metlov and Y. P. Lee, "Map of metastable states for thin circular magnetic nanocylinders," Appl. Phys. Lett. **92**, 112506 (2008).

[21] S.-H. Chung, R. D. McMichael, D. T. Pierce, and J. Unguris, "Phase diagram of magnetic nanodisks measured by scanning electron microscopy with polarization analysis," Phys. Rev. B **81**, 024410 (2010).

[22] N. D. Mermin, "The topological theory of defects in ordered media," Rev. Mod. Phys. **51**, 591–648 (1979).

[23] K. Yu. Guslienko, V. Novosad, Y. Otani, H. Shima, and K. Fukamichi, "Magnetization reversal due to vortex nucleation, displacement, and annihilation in submicron ferromagnetic dot arrays," Phys. Rev. B **65**, 024414

(2001).

[24] K. S. Buchanan, M. Grimsditch, F. Y. Fradin, S. D. Bader, and V. Novosad, "Driven Dynamic Mode Splitting of the Magnetic Vortex Translational Resonance," Phys. Rev. Lett. **99**, 267201 (2007).

[25] O. V. Sukhostavets, B. Pigeau, S. Sangiao, G. de Loubens, V. V. Naletov, O. Klein, K. Mitsuzuka, S. Andrieu, F. Montaigne, and K. Y. Guslienko, "Probing the anharmonicity of the potential well for a magnetic vortex core in a nanodot," Phys. Rev. Lett. **111**, 247601 (2013).

[26] E. Holmgren, A. Bondarenko, M. Persson, B. A. Ivanov, and V. Korenivski, "Transient dynamics of strongly coupled spin vortex pairs: Effects of anharmonicity and resonant excitation on inertial switching," Appl. Phys. Lett. **112**, 192405 (2018).

[27] V. Novosad, K. Yu. Guslienko, H. Shima, Y. Otani, S. G. Kim, K. Fukamichi, N. Kikuchi, O. Kitakami, and Y. Shimada, "Effect of interdot magnetostatic interaction on magnetization reversal in circular dot arrays," Phys. Rev. B **65**, 060402 (2002).

[28] K. Y. Guslienko, G. N. Kakazei, J. Ding, X. M. Liu, and A. O. Adeyeye, "Giant moving vortex mass in thick magnetic nanodots," Sci. Rep. **5**, 13881 (2015).

[29] R. V. Verba, A. Hierro-Rodriguez, D. Navas, J. Ding, X. M. Liu, A. O. Adeyeye, K. Y. Guslienko, and G. N. Kakazei, "Spin-wave excitation modes in thick vortex-state circular ferromagnetic nanodots," Phys. Rev. B **93**, 214437 (2016).

[30] S. S. Cherepov, B. C. Koop, A. Yu. Galkin, R. S. Khymyn, B. A. Ivanov, D. C. Worledge, and V. Korenivski, "Core-core dynamics in spin vortex pairs," Phys. Rev. Lett. **109**, 097204 (2012).

[31] M. Yan, H. Wang, and C.E. Campbell, "Unconventional magnetic vortex structures observed in micromagnetic simulations," J. Magn. Magn. Mater. **320**, 1937–1944 (2008).

[32] G. Siracusano, R. Tomasello, A. Giordano, V. Puliafito, B. Azzerboni, O. Ozatay, M. Carpentieri, and G. Finocchio, "Magnetic radial vortex stabilization and efficient manipulation driven by the Dzyaloshinskii-Moriya interaction and spin-transfer torque," Phys. Rev. Lett. **117**, 087204 (2016).

[33] C. Phatak, A. K. Petford-Long, and O. Heinonen, "Direct observation of unconventional topological spin structure in coupled magnetic discs," Phys. Rev. Lett. **108**, 067205 (2012).

[34] S. Wintz, C. Bunce, A. Neudert, M. Körner, T. Strache, M. Buhl, A. Erbe, S. Gemming, J. Raabe, C. Quitmann, and J. Fassbender, "Topology and origin of effective spin meron pairs in ferromagnetic multilayer elements," Phys. Rev. Lett. **110**, 177201 (2013).

[35] F. Garcia-Sanchez, J. Sampaio, N. Reyren, V. Cros, and J.-V. Kim, "A skyrmion-based spin-torque nano-oscillator," New J. Phys. **18**, 075011 (2016).

[36] A. Vansteenkiste, J. Leliaert, M. Dvornik, M. Helsen, F. Garcia-Sanchez, and B. Van Waeyenberge, "The design and verification of MuMax3," AIP Advances **4**, 107133 (2014).

[37] J. Gräfe, M. Weigand, N. Träger, G. Schütz, E. J. Goering, M. Skripnik, U. Nowak, F. Haering, P. Ziemann, and U. Wiedwald, "Geometric control of the magnetization reversal in antidot lattices with perpendicular magnetic anisotropy," Phys. Rev. B **93**, 104421 (2016).

[38] M Krupinski, D Mitin, A Zarzycki, A Szkudlarek, M Giersig, M Albrecht, and M Marszałek, "Magnetic transition from dot to antidot regime in large area Co/Pd nanopatterned arrays with perpendicular magnetization," Nanotechnology **28**, 085302 (2017).

[39] G. N. Kakazei, M. Ilyn, O. Chubykalo-Fesenko, J. Gonzalez, A. A. Serga, A. V. Chumak, P. A. Beck, B. Laegel, B. Hillebrands, and K. Y. Guslienko, "Slow magnetization dynamics and energy barriers near vortex state nucleation in circular permalloy dots," Appl. Phys. Lett. **99**, 052512 (2011).

[40] G. A. Melkov, Y. Kobljanskyj, V. Novosad, A. N. Slavin, and K. Y. Guslienko, "Probing the energy barriers in nonuniform magnetization states of circular dots by broadband ferromagnetic resonance," Phys. Rev. B **88**, 220407 (2013).

[41] G. de Loubens, A. Riegler, B. Pigeau, F. Lochner, F. Boust, K. Y. Guslienko, H. Hurdequint, L. W. Molenkamp, G. Schmidt, A. N. Slavin, V. S. Tiberkevich, N. Vukadinovic, and O. Klein, "Bistability of Vortex Core Dynamics in a Single Perpendicularly Magnetized Nanodisk," Phys. Rev. Lett. **102**, 177602 (2009).

[42] J. Ding, G. N. Kakazei, X. Liu, K. Y. Guslienko, and A. O. Adeyeye, "Higher order vortex gyrotropic modes in circular ferromagnetic nanodots," Sci. Rep. **4**, 4796 (2014).